Two-Dimensional Array of Poly(methacrylic acid) Brushes on Gold Substrates. Interaction with Ferrocene-Terminated Poly(oxyethylene)s

Masazo Niwa,* Toshiaki Mori, and Nobuyuki Higashi

Department of Molecular Science & Technology, Faculty of Engineering, Doshisha University, Tanabe, Kyoto 610-03, Japan

Received April 28, 1995; Revised Manuscript Received August 8, 1995[⊗]

ABSTRACT: Polymeric amphiphiles ($\mathbf{1}_n$), consisting of a poly(methacrylic acid) (PMAA) segment (segment length, n = 35 and 63) and two long alkyl chains whose ends are modified with disulfide, form self-assembled monolayers on gold electrodes. The lateral molecular distribution within the monolayers is successfully controlled by varying the conformational size of the PMAA segments during assembling. Ferrocene-terminated poly(oxyethylene)s ($\mathbf{2}_m$), having various chain lengths (m = 10−120) are prepared and used as guest polymers. Host−guest interactions of $\mathbf{2}_m$ and the $\mathbf{1}_n$ monolayer-covered gold electrodes can be monitored electrochemically by means of electron transfer of the ferrocene moiety. The amount of adsorbed $\mathbf{2}_m$ gives a maximum when the chain length of guest $\mathbf{2}_m$ (m) matches that of host $\mathbf{1}_n$ monolayer (n). When the lateral molecular distribution in the monolayer brushes is controlled to be most favorable for the guest polymers, a 1:1 host−guest polymer complexation can be accomplished. FTIR spectroscopic data suggest that such complexation results from multiple hydrogen bonding between the COOH groups and the ether oxygen atoms.

Introduction

The interaction between two different macromolecules plays a key role in living systems since biological phenomena such as enzymatic processes, protein syntheses, and molecular recognition on the biomembrane surfaces are indebted principally to specific intermacromolecular interactions and to structural features of the resultant macromolecular assemblies. Organized monolayers provide peculiar environments for molecular interactions and, consequently, for molecular recognition. Novel molecular recognition systems can be developed by using molecular assemblies, which may possess characteristics different from those in bulk phases. From this point of view, we have devised a strategy in which polymeric amphiphiles carrying a purely synthetic polyelectrolyte segment such as poly(methacrylic acid) (PMAA) are aligned on a water surface.[1,2] These polymer assemblies have shown unique properties; for instance, the surface monolayers of PMAA-based amphiphiles were found to have the ability to read out the chain length of poly(oxyethylene) (POE) added in the water subphase on the basis of surface pressure−area isotherm measurements.

We report herein a specific adsorption of POEs ($\mathbf{2}_m$, m = 10−120) at self-assembled monolayers of PMAA-based amphiphiles ($\mathbf{1}_n$, n = 35 and 63) on gold electrodes. Self-assembled monolayers have been reported to be readily prepared on gold by spontaneous adsorption of organic thiols and disulfides.[3−11] We have already established that self-assembled monolayers of $\mathbf{1}_n$ are formed spontaneously on gold substrates from aqueous solutions, and then the packing density of $\mathbf{1}_n$ within the monolayers is successfully controlled based upon the conformational size of the PMAA segment adopted during adsorption (see Figure 1).[12,13]

One terminus of the POE chains as a guest polymer is labeled with ferrocene as a redox-active moiety to detect electrochemically the amount of POE adsorbed on $\mathbf{1}_n$ monolayers. Figure 2 shows chemical structures of the host polymer monolayers ($\mathbf{1}_n$) and the guest polymers ($\mathbf{2}_m$) used in this study.

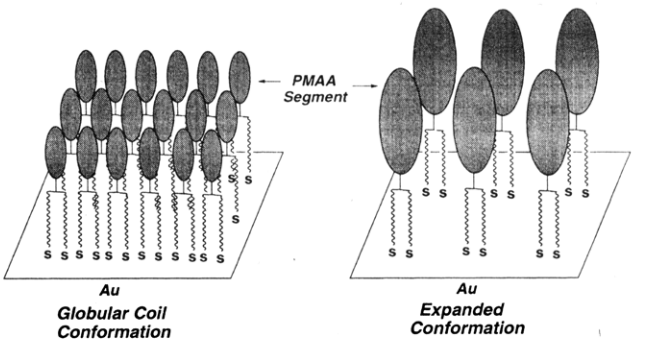

Figure 1. Schematic model for two-dimensional molecular distribution within the monolayers on gold substrates by taking advantage of the conformational size of a poly(methacrylic acid) segment adopted during adsorption.

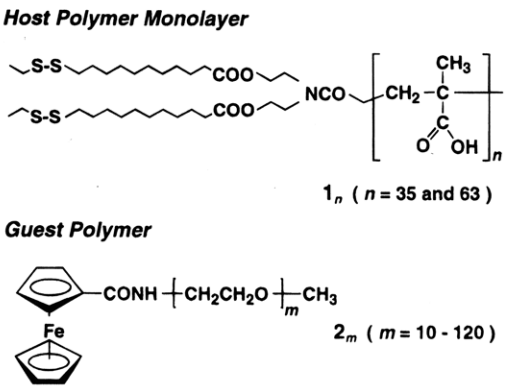

Figure 2. Chemical structures of host polymer monolayers and guest polymers.

Experimental Section

Materials. Preparation of $\mathbf{1}_n$. The preparation of the polymeric amphiphiles $\mathbf{1}_n$ with different PMAA segment lengths (n = 32 and 63) has been described elsewhere.[12]

Preparation of Ferrocene-Terminated POEs ($\mathbf{2}_m$). Ferrocene-terminated POEs were prepared in a manner similar

[⊗] Abstract published in *Advance ACS Abstracts,* October 15, 1995.

0024-9297/95/2228-7770$09.00/0

to that of Murray et al.[14] ω-Hydroxy-α-methoxypoly(oxyethylene)s with various chain lengths (number-average degree of polymerization, m = 10−120) were kind gifts from Japan Catalytic Chemical Industry Co., Ltd.

Preparation of Monolayers on Gold Substrates. Monolayers were spontaneously formed by immersing gold mirror plates, which were prepared by evaporation of gold onto glass plates, or clean gold electrodes into a 1 mM solution of $\mathbf{1}_n$ in water (purified with a Milli-Q. purification system, Millipore) with a prescribed pH. After a 10-h immersion that was enough to reach a steady-state monolayer formation,[12] the gold substrates were removed and rinsed with clean water.

Adsorption of $\mathbf{2}_m$ onto $\mathbf{1}_n$ monolayers. The adsorption experiment of $\mathbf{2}_m$ onto $\mathbf{1}_n$ monolayers was carried out by immersing the $\mathbf{1}_n$-modified plates or electrodes in aqueous solutions of $\mathbf{2}_m$ (1 unit mM) and allowing 2 h for equilibration. The pH of the solutions was kept at 4.0 during the adsorption experiment since the COOH groups in the PMAA segment were protonated in that pH region. After equilibration, the substrates were washed with a water of pH 4.0 to remove free $\mathbf{2}_m$'s.

Electrochemical Measurements. Cyclic voltammetry was performed with a CV-1B (BAS) and an RW-21 X−Y recorder (Rikadenki, Tokyo). The gold electrodes were mounted in a conventional three-electrode cell with an exposed area of 0.02 cm^2. Solutions were purged with nitrogen. All potentials were measured and reported with respect to a Ag/AgCl (saturated KCl) reference electrode. Solutions were prepared immediately before use with deionized water from a Milli-Q purification system. pH's of the solutions were adjusted with the required amount of HCl and NaOH. KCl and $[Ru(NH_3)_6]Cl_3$, as an electrolyte and a redox probe, respectively, were reagent grade.

Spectroscopic Measurements. X-ray photoelectron spectra (XPS) for the $\mathbf{2}_m$-bound $\mathbf{1}_n$ monolayers on gold plates were measured by a Shimadzu ESCA-1000 system with a Mg Kα X-ray source at a take-off angle of 30°. The charging shift was corrected with the C_{1s} line emitted from neutral hydrocarbon.

FTIR (reflection−absorption) spectra for the same monolayers on gold plates were measured by a Nicholet System 800 using a reflection attachment at the incident angle of 80°, together with a polarizer.

Results and Discussion

Lateral Molecular Distribution within the $\mathbf{1}_n$ Monolayers on Gold Electrodes. It is important to elucidate a molecular distribution within the $\mathbf{1}_n$ monolayers. For that purpose, we employed a disk-shaped microelectrode model[12,15,16] as shown schematically in Figure 3. Quantitative information about the molecular distribution can be extracted by fitting the voltammograms with the theoretical treatment of such a model. $Ru(NH_3)_6^{3+/2+}$ was used as a reference redox couple for probing the active sites in a monolayer. In this model, the electrode is assumed to be covered with disk-shaped active sites with an average radius of R_a and an area fraction of $1 - \theta$ (where θ is the fractional coverage of an inactive (blocking) site). Each active site is surrounded by an inactive area with an average radius of R_0; hence, the distance between active sites is $2R_0$. For small area fractions of active sites, R_a and R_0 are related to $1 - \theta$ by

$$1 - \theta = R_a^2/R_0^2 \qquad (1)$$

Figure 3 displays the results of simulation of a microarray electrode cyclic voltammetry for $\mathbf{1}_{63}$ monolayer-covered electrodes prepared at different pHs. The detailed procedures have been described elsewhere.[12] With elevating pH, the area fraction of active sites ($1 - \theta$) increases steeply at pH ~5, which corresponds well to that of the conformational transition of PMAA in

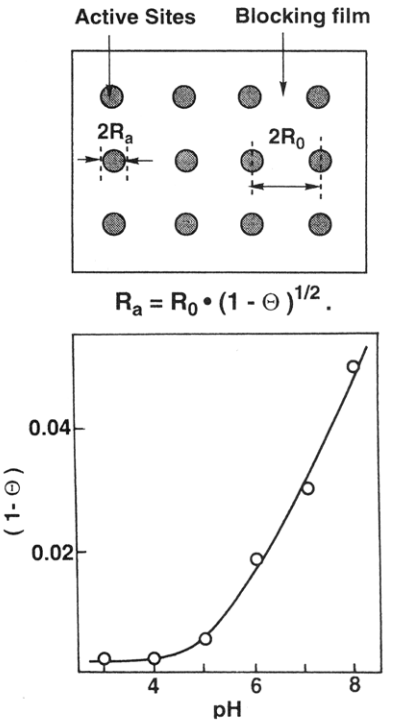

Figure 3. Disk-shaped microelectrode model[12,15,16] (top). Relationship between the fraction of active sites ($1 - \theta$) and pH at which each monolayer was prepared (bottom).

solution.[17] These results demonstrate that the active site areas in the monolayers are readily controlled by taking advantage of the conformational change of the PMAA segment induced by the surrounding pH.

By using these parameters, one can also estimate an apparent surface coverage of $\mathbf{1}_n$ (Γ_1, mol cm^{-2}) on the electrodes. When the surface coverage Γ_1 is assumed to be equal to the occupied area of the PMAA segment, $1 - \theta$ is related to Γ_1 by

$$\Gamma_1 = (1 - \theta)/\pi s^2 N_A \qquad (2)$$

where s and N_A are the radius of gyration of the PMAA segment[18] and Avogadro's number, respectively. For the monolayers of $\mathbf{1}_{63}$ and $\mathbf{1}_{35}$ prepared at pH 6.0, surface coverages were computed by the use of eq 2 to be $\Gamma_1 = 4.1 \times 10^{-12}$ and $\Gamma_1 = 6.0 \times 10^{-12}$, respectively, where the cyclic voltammetric curves for estimation of $1 - \theta$ were obtained at pH 4.0.

Interaction of $\mathbf{1}_n$ Monolayer-Immobilized Gold Electrodes with Guest $\mathbf{2}_m$'s. To examine the interaction of the $\mathbf{1}_n$ monolayers and the guest $\mathbf{2}_m$'s, we prepared monolayers on clean gold electrodes from aqueous solutions containing $\mathbf{1}_n$ at pH 6.0. Adsorption experiments of $\mathbf{2}_m$ were performed by immersing the $\mathbf{1}_n$ monolayer-modified electrodes thus obtained into aqueous solutions of $\mathbf{2}_m$ and allowing 2 h for equilibration. The pH of the solutions was kept at 4.0 during the experiment since the COOH groups in the PMAA segments were protonated in that pH region. After equilibration, the electrodes were washed with a water of pH 4.0 to remove free guest polymers. Figure 4A shows a typical cyclic voltammogram obtained for $\mathbf{2}_{46}$ adsorbed on the $\mathbf{1}_{63}$-modified electrode with 0.1 M KCl as an electrolyte at pH 4.0. The peaks are due to the one-electron oxidation and reduction of the ferrocene moiety of adsorbed $\mathbf{2}_{46}$. Rinsing the electrode with a water of pH 4.0 four additional times resulted in nearly identical voltammograms, which implies that desorption

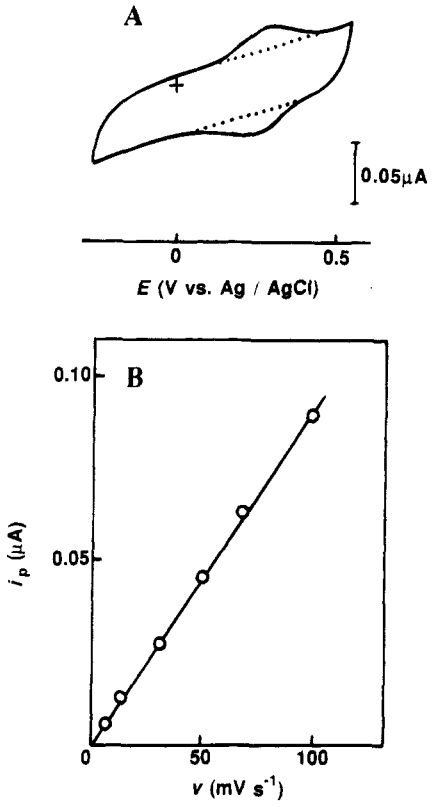

Figure 4. (A) Cyclic voltammograms acquired at a scan rate of 100 mV s^{-1} of a $\mathbf{1}_{63}$ monolayer-covered gold electrode (dotted line) and the same electrode after adsorption of $\mathbf{2}_{46}$ on the $\mathbf{1}_{63}$ monolayer (solid line). In both cases, the supporting electrolyte is 0.1 M KCl at pH 4.0. (B) Plot of peak current (i_p) vs scan rate (v). Solution conditions are the same as in (A). Electrode area 0.02 cm^2.

is negligible. Figure 4B displays a plot of the peak current (i_p) of this electrode obtained at different potential scan rate against scan rate (v). The peak current is found to vary linearly with scan rate. This indicates that $\mathbf{2}_{46}$ is surface-bound to the $\mathbf{1}_{63}$ monolayer and is not subjected to diffusion to the electrode. From these voltammetric data, we attempted to estimate the electron-transfer (ET) distance (d). Peak separations in Figure 4A were used to calculate an apparent ET rate constant (k_{ET}) of 2.6 s^{-1}.[19] Using the conventional expression,[19] $k_{ET} = \nu \exp[-\beta(d - d_0)] \exp(-\Delta G^*/RT)$, with $\nu = 10^{13}$ s^{-1},[20a] $\beta = 1.2$ $Å^{-1}$,[20b] $d_0 = 3.3$ Å,[20a] and $\Delta G^* = 11$ kJ mol^{-1},[21] we calculate an ET distance of d = 24 Å, which agrees well with the ellipsometric thickness of the PMAA segment-free, **3** monolayer (23

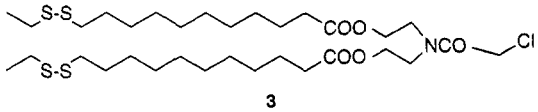

3

± 1 Å) that was determined previously.[12] The PMAA segment adopts a relatively hydrophobic hypercoiled conformation at pH 4.0. Thus, the $\mathbf{1}_{63}$ monolayer surface would be considered to provide a hydrophobic environment for the approaching guest polymers. The ferrocene group is more hydrophobic than the other portion of a $\mathbf{2}_m$ molecule such as a POE segment. We suppose, thus, that the ferrocene groups must exist near the connector moiety of $\mathbf{1}_{63}$, where the PMAA segment is joined with two long alkyl chains and ET can occur.

When the $\mathbf{2}_{46}/\mathbf{1}_{63}$ electrode was treated with water at pH 8.0, at which the COOH groups of the $\mathbf{1}_{63}$ layer are

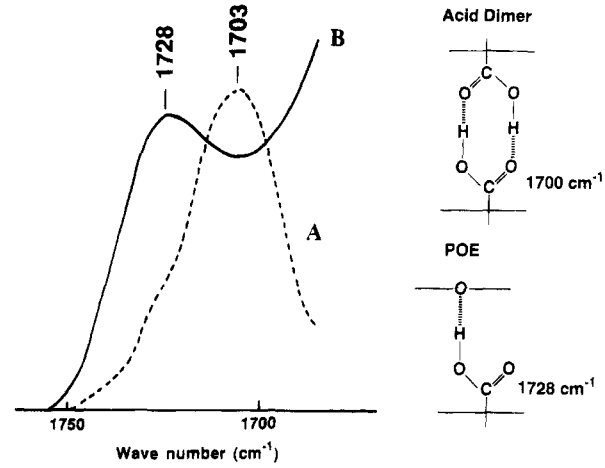

Figure 5. High-resolution FTIR reflection absorption spectra in the C=O stretching band region for $\mathbf{1}_{63}$ monolayer (A) and $\mathbf{2}_{46}/\mathbf{1}_{63}$ complexed monolayer (B) on gold plates.

completely deprotonated, i.e., they exist as a carboxylate anion, the redox peaks disappeared from the voltammogram. This means that the complexation of $\mathbf{2}_{46}$ and $\mathbf{1}_{63}$ was inhibited and then the free $\mathbf{2}_{46}$ diffused far from the monolayer electrode where ET no longer could occur. The binding of $\mathbf{2}_{46}$ to the $\mathbf{1}_{63}$ monolayer is, therefore, supposed to stem mainly from multiple hydrogen bonding between COOH groups in $\mathbf{1}_{63}$ and ether oxygen atoms in $\mathbf{2}_{46}$. To obtain more direct evidence for such complexation, FTIR reflection absorption spectra were measured for the monolayers on gold plates.

Figure 5 shows FTIR spectra of a pure $\mathbf{1}_{63}$ monolayer (A) and a $\mathbf{2}_{46}/\mathbf{1}_{63}$ complex monolayer (B). We focused on absorptions in the C=O stretching region. A characteristic feature of the spectrum of the pure $\mathbf{1}_{63}$ monolayer is the presence of an infrared bond at 1703 cm^{-1} which is assigned to the carboxylic acid dimer.[22] Though the molecule of $\mathbf{1}_{63}$ has two ester groups in its hydrophobic portion, the content of them is much smaller compared with that of the COOH group and thus the absorption band based upon ester carbonyl (at ~1730 cm^{-1}) may be too weak to appear in the spectrum. In the spectrum of complexed $\mathbf{2}_{46}/\mathbf{1}_{63}$ monolayer, a new band appeared at 1728 cm^{-1} together with a minor band due to the carboxylic acid dimer at 1703 cm^{-1}. The band at 1728 cm^{-1} is assigned to free C=O groups[22] that occur when intermolecular hydrogen bonds are formed between the COOH groups of the PMAA segment and the ether oxygen atoms of the POE chains as depicted in Figure 5. These spectroscopic data clearly demonstrate that a main driving force for complexation between the host monolayer and the guest polymer stems from a multiple hydrogen bonding of $COOH\cdots OCH_2CH_2$.

Chain Length Recognition of Guest Polymers $\mathbf{2}_m$ by $\mathbf{1}_n$ Monolayer-Immobilized Electrodes. The ferrocene-terminated POEs, $\mathbf{2}_m$ having various chain lengths in the range m = 10−120, were used to elucidate the chain length effects of $\mathbf{2}_m$ on electrochemical responses of $\mathbf{1}_n$ (n = 35 and 63) monolayer-immobilized electrodes. The amount of $\mathbf{2}_m$ absorbed on $\mathbf{1}_n$ monolayers can be evaluated on the basis of cyclic voltammograms for each combination of $\mathbf{1}_n$ and $\mathbf{2}_m$ as follows. Surface coverages (Γ_2, mol cm^{-2}) of $\mathbf{2}_m$ bound to the $\mathbf{1}_n$ layer were first estimated by integration of the charge beneath the voltammetric peaks. The surface coverages (Γ_1) of $\mathbf{1}_n$ on the naked gold electrodes at pH 6.0 were evaluated electrochemically by using $Ru(NH_3)_6^{3+/2+}$ as

Table 1. Surface Coverages of 1_n Monolayers on Gold Electrodes (Γ_1) and 2_m Bound to the 1_n Monolayer-Covered Gold Electrodes (Γ_2)

chain length of 2_m	Γ_2[a] × 10^{12} (mol cm^{-2})		Γ_2/Γ_1	Γ_2/Γ_1
	1_{35}[b]	1_{63}[b]	(n = 35)	(n = 63)
10	18.3	10.0	3.1	2.5
23	8.9	4.8	1.5	1.2
46	4.3	2.6	0.72	0.64
86	1.6	1.0	0.27	0.24
120		0.55		0.14

[a] Surface coverages of 2_m bound to 1_n monolayer-covered electrodes. [b] Surface coverages of 1_n monolayers on electrodes, calculated by eq 2 as described in the text. For 1_{35}, $\Gamma_1 = 6.0 \times 10^{-12}$; for 1_{63}, $\Gamma_1 = 4.1 \times 10^{-12}$.

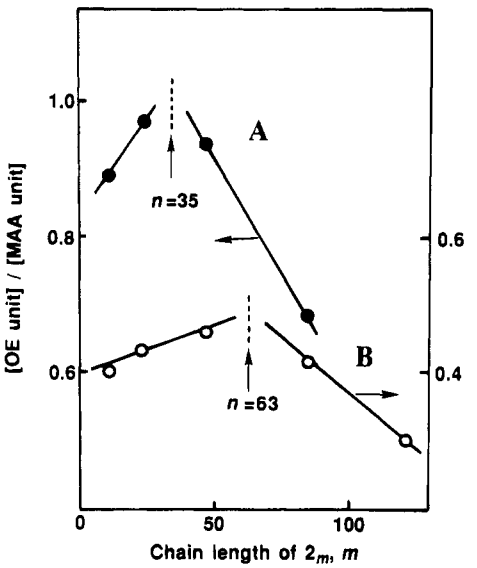

Figure 6. Relationship between the ratio of oxyethylene units of the 1_n monolayer-bound 2_m ([OE unit]) to methacrylic acid unit of the 1_n monolayer ([MAA unit]) and the chain length of 2_m (m) for the cases of a 1_{35} monolayer (A) and a 1_{63} monolayer (B).

a redox couple on the assumption of a disk-shaped microelectrode model[12,15,16] as described above. The values of Γ_1 and Γ_2 thus obtained for each 1_n (n = 35 and 63)-immobilized electrode are summarized in Table 1. By using the values of Γ_1 and Γ_2, the ratios of Γ_2/Γ_1 were calculated and listed also in Table 1. The ratios (Γ_2/Γ_1) for both cases of 1_{35} and 1_{63} monolayers are found to decrease with increasing chain length of $2_m(m)$, implying that the monolayers capture preferably the guest polymers having a shorter chain length (m). To reveal more quantitative stoichiometry for such complexation, the ratios ([OE unit]/[MAA unit]) of the number of repeating units for each polymer segment ([OE unit] for 2_m or [MAA unit] for 1_n) were calculated from values of Γ_2 and Γ_1 with the following equation: [OE unit]/[MAA unit] = $(m\Gamma_2)/(n\Gamma_1)$ and plotted against the chain length (m) of 2_m in Figure 6. As can be seen from the figure, the ratios ([OE unit]/[MAA unit]) for both monolayers of 1_{35} and 1_{63} increase systematically with an increase in the chain length (m) of guest polymers up to when m is almost equal to the segment length (n) of the host monolayers, beyond which the ratios show a tendency to decrease. In the case of $m < n$, the segment–segment interactions may not be so strong to form a stoichiometric complex between the repeating units although the monolayers captured relatively more guest molecules, as mentioned above. On the other hand, a guest polymer having a much longer chain length compared with the segment length

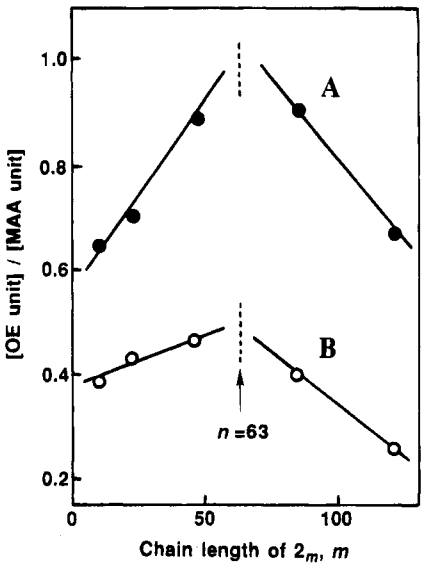

Figure 7. Plots of the ratio of [OE unit]/[MAA unit] against the chain length of 2_m (m) for the cases of 1_{63} monolayers prepared from aqueous solutions of pH's 8.0 (A) and 6.0 (B).

of the monolayer prefers existing in bulk aqueous phase to complexing with the monolayer probably due to the hydrophilicity of the long, free segment, consequently depressing such complexation. A most effective intermacromolecular hydrogen bonding is supposed to work when the segment length of monolayers (n) is matched with that of the corresponding guest polymers (m); in other words, the monolayers of 1_{35} and 1_{63} have the ability to read out the chain length of 2_m. The ratio of [OE unit]/[MAA unit] at maximum for the 1_{63} monolayer is, however, considerably lower than unity, whereas the ratio for 1_{35} monolayer is almost unity. This suggests that a molecular space of 1_{63} monolayer having a longer PMAA segment is not enough to accept the guest polymer in comparison with that of the shorter PMAA segment-carrying 1_{35} monolayer. If so, it would be expected that the monolayer with a looser molecular distribution can give a more appropriate space for capturing the guest polymer. The monolayer of 1_{63} was thus prepared on an electrode at pH 8.0, at which the PMAA segment is in an expanded form. The lateral molecular packing within the resultant monolayer should become looser. The result is plotted in Figure 7 in the same way in Figure 6. The chain length of 2_m at a maximum ratio of [OE unit]/[MAA unit] is again very consistent with that of the 1_{63} monolayer, and in addition, the value of maximum ratio increases compared with that of the monolayer prepared at pH 6.0 and becomes close to unity.

To obtain information regarding the composition of these complexed monolayers, XPS spectroscopy was performed for a typical sample of the $2_{46}/1_{63}$ complexed monolayer, whose ratio of [OE unit]/[MAA unit] is 0.89 as estimated electrochemically (see Figure 7). The spectrum of the carbon 1s region is displayed in Figure 8. The spectrum is found to be composed of four components: ferrocenyl carbon, neutral carbon, etheral carbon, and carboxylic acid carbon at 284.4, 285.4, 286.4, and 287.2 eV, respectively, on the basis of computer-generated peak fits using Gaussian peak shapes. The peak area gives atomic composition for each component. By using the peak areas of etheral carbon and carboxylic acid carbon, the ratio of [OE unit]/[MAA unit] was calculated, giving [OE unit]/[MAA unit] = 0.93, in close

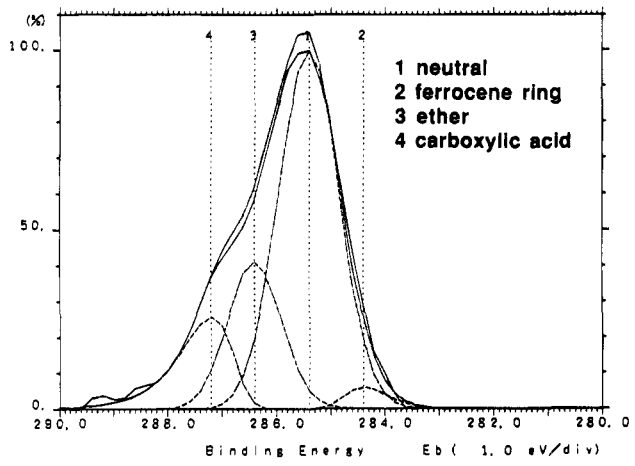

Figure 8. XPS spectrum in the carbon 1s region of the $\mathbf{2}_{46}/\mathbf{1}_{63}$ complexed monolayer on a gold plate. Broken lines represent computer-generated peak fits using Gaussian peak shapes.

agreement with that (0.89) evaluated using electron transfer of the ferrocene group.

Finally, the reversibility of the complexation was examined electrochemically for the same complexed monolayer ($\mathbf{2}_{46}/\mathbf{1}_{63}$). When the complexed monolayer electrode was immersed into water of pH 8.0, the redox peaks of ferrocene moiety of $\mathbf{2}_{46}$ disappeared rapidly and the ratio of [OE unit]/[MAA unit] became close to zero, implying that the complexation of $\mathbf{2}_{46}$ with $\mathbf{1}_{63}$ monolayer was weakened upon breaking the hydrogen bonds ($COOH\cdots OCH_2CH_2$) due to deprotonation of the COOH group of the PMAA segment. Upon immersing this electrode into aqueous solution containing $\mathbf{2}_{46}$ at pH 4.0, the redox peaks appeared again and then the ratio of [OE unit]/[MAA unit] reverted completely to the original value. These results clearly demonstrate that the $\mathbf{1}_n$ monolayer can adsorb and desorb the guest polymer $\mathbf{2}_m$ reversibly by changing the surrounding pH while maintaining a chain length recognition ability.

Conclusions

The present study demonstrates that (i) interaction of $\mathbf{1}_n$ monolayer-covered electrodes with $\mathbf{2}_m$'s can be estimated on the basis of electron transfer of their ferrocene moieties, (ii) the main driving force of such host–guest polymer complexation is due to multiple hydrogen bonding between COOH groups and ether oxygen atoms, (iii) $\mathbf{1}_n$ monolayers have the ability to read out the chain length of guest $\mathbf{2}_m$'s, and (iv) the amount of captured guest polymers can be controlled by a molecular distribution within host $\mathbf{1}_n$ monolayers that is changeable based upon conformational size of the PMAA segment. We believe that these findings provide a first example of the polyelectrolyte assembly which can recognize the different macromolecules and that this system is of particular significance in view of its applicability not only for a polymer sensor but also for the model of a biofunctional polymer.

References and Notes

(1) (a) Niwa, M.; Katsurada, N.; Higashi, N. *Macromolecules* **1988**, *21*, 1878. (b) Niwa, M.; Hayashi, T.; Higashi, N. *Langmuir* **1990**, *6*, 263. (c) Higashi, N.; Shiba, H.; Niwa, M. *Macromolecules* **1989**, *22*, 4650. (d) Higashi, N.; Shiba, H.; Niwa, M. *Macromolecules* **1990**, *23*, 5297. (e) Higashi, N.; Matsumoto, T.; Niwa, M. *J. Chem. Soc., Chem. Commun.* **1991**, 1517. (f) Higashi, N.; Nojima, T.; Niwa, M. *Macromolecules* **1991**, *24*, 6549. (g) Higashi, N.; Shimoguchi, M.; Niwa, M. *Langmuir* **1992**, *8*, 1509. (h) Higashi, N.; Matsumoto, T.; Niwa, M. *Langmuir* **1994**, *10*, 4651.
(2) Niwa, M.; Shimoguchi, M.; Higashi, N. *J. Colloid Interface Sci.* **1992**, *145*, 592.
(3) Nuzzo, R. G.; Allara, D. L. *J. Am. Chem. Soc.* **1983**, *105*, 4481.
(4) Li, T. T.-T.; Weaver, M. J. *J. Am. Chem. Soc.* **1984**, *106*, 6107.
(5) Maoz, R.; Sagiv, J. *Langmuir* **1987**, *3*, 1034.
(6) Bain, C. C.; Evall, J.; Whitesides, G. M. *J. Am. Chem. Soc.* **1989**, *111*, 7155.
(7) Widrig, C. D.; Alves, C. A.; Porter, M. D. *J. Am. Chem. Soc.* **1991**, *113*, 2805.
(8) Collard, D. M.; Fox, M. A. *Langmuir* **1991**, *7*, 1192.
(9) Higashi, N.; Mori, T.; Niwa, M. *J. Chem. Soc., Chem. Commun.* **1990**, 225.
(10) Niwa, M.; Mori, T.; Higashi, N. *J. Mater. Chem.* **1992**, *2*, 245.
(11) Niwa, M.; Mori, T.; Nishio, E.; Nishimura, H.; Higashi, N. *J. Chem. Soc., Chem. Commun.* **1992**, 547.
(12) Niwa, M.; Mori, T.; Higashi, N. *J. Chem. Soc., Chem. Commun.* **1993**, 1081.
(13) Niwa, M.; Mori, T.; Higashi, N. *Macromolecules* **1993**, *26*, 1936.
(14) Pinkerton, M. J.; Mest, Y. L.; Zhang, H.; Watanabe, M.; Murray, R. W. *J. Am. Chem. Soc.* **1990**, *112*, 3730.
(15) Amatore, C.; Savéant, J. M.; Tessier, D. J. *Electroanal. Chem.* **1989**, *147*, 39.
(16) Finklea, H. O.; Snider, D. A.; Fedyk, J. *Langmuir* **1990**, *6*, 371.
(17) Olea, A. F.; Thomas, J. K. *Macromolecules* **1989**, *22*, 1165, and references therein.
(18) Oth, A.; Doty, P. *J. Phys. Chem.* **1952**, *56*, 43.
(19) Laviron, E. *J. Electroanal. Chem.* **1979**, *101*, 19.
(20) (a) Marcus, R. A.; Sutin, N. *Biochim. Biophys. Acta* **1985**, *811*, 265. (b) Gray, H. B.; Malmstrom, B. *Biochemistry*, **1989**, *28*, 7499.
(21) Tarlov, M. J.; Bowden, E. F. *J. Am. Chem. Soc.* **1991**, *113*, 1847.
(22) Lee, J. Y.; Painter, P. C.; Coleman, M. M. *Macromolecules* **1988**, *21*, 346.

MA950575U